

Non-equilibrium Gas Discharge Conditions for Origin of Life and Living Matter. Experiments of Miller. Modeling of the Conditions with Gas Coronal Discharge Simulating Primary Atmosphere

Ignat Ignatov^{1*} Oleg Mosin²

1. DSc, Professor, Scientific Research Center of Medical Biophysics (SRCMB),

N. Kopernik Street, 32, Sofia 1111, Bulgaria

2. PhD (Chemistry), Biotechnology Department, Moscow State University of Applied Biotechnology,

Talalikhina Street, 33, Moscow 109316, Russian Federation

* E-mail of the corresponding author: mbioph@dir.bg

Abstract

In this paper are submitted data on the possibility of applying the Coronal gas discharge effect in modeling non-equilibrium conditions with gas electric discharge simulating conditions occurring in the primary atmosphere (electric sparks, lightning). The physical basis and technique of visualization of gas discharge (GD) glowing of water drops in alternating electric fields of high electrical voltage (5–30 kV) and frequency (10–150 kHz) as well as possible electrosynthesis of organic molecules from a mixture of inorganic substances as hydrogen (H₂), methane (CH₄), ammonia (NH₃) and carbon monoxide (CO) in aqueous solutions of water exposed under electrical discharge, UV-radiation and thermal heating was examined. The colour coronal spectral gas discharge analysis, IR-spectroscopy, and NES-, and DENS-methods were applied for investigation of water samples of various origin, the samples of hot mineral, sea and mountain water obtained from various sources of Bulgaria, as well as cactus juice and Mediterranean jellyfish *Cotylorhiza tuberculata* obtained from Aegean Sea (Chalkida, Greece). As a main parameter was measured the average energy of hydrogen bonds between H₂O molecules and in the process of cluster formation (dimer, trimer) and the function of the distribution of energies Δf between individual H₂O molecules compiles -0.1067 ± 0.0011 eV. These data indicate that the origination of life and living matter depends on the structural and physical chemical properties of water, as well as the temperature and pH value.

Key words: Color gas discharge effect, IR-spectroscopy, primary atmosphere, water, origin of life, S. Miller's experiments.

1. Introduction

Coronal gas discharge effect (CGDE) is observed by the characteristic glowing of corona electrical discharge (flooding, crown, streamer) on the surface of objects being placed in the alternating electric field of high frequency (10–150 kHz) and electric voltage (5–30 kV) (Kilrian, 1949). In this process in the ionization zone develops the corona gas discharge sliding on the dielectric surface, occurring in a nonuniform electric field near the electrode having a small radius of curvature (Kirlian, 1949). With decreasing in the degree of heterogeneity of the electric field (the radius of curvature of the electrode ~ 1–3 mm) and with increasing of electric voltage the corona electrical discharge takes not uniform, but streamer (sometimes flare or spray) form. In this case, the electrically active processes are removed off at a distance of 10-20 cm from the surface of the electrode.

In the scientific literature, along with the terms of coronal gas discharge (CGD) are used gas discharge (GD), electric frequency (EFD) discharge, selective high frequency electric (SHFED) discharge etc. (Antonov & Yuskeselieva, 1968; Antonov & Yuskeselieva, 1985).

Coronal gas discharge glowing has found some scientific and practical applications in biophysics, as well as other branches of science (Gudakova, 1988) and technology (Lapitskiy & Pesotskaya, 2012). Its advantages include safety, sterility, clarity and interpretability of the data obtained, ease of storage and subsequent computer processing, the ability to monitor the development of processes in time, comparing the structural, functional and temporal processes, etc.

Scientific and fundamental aspects of the coronal gas discharge effect and its scientific value consists in the fact that the CGD creates in laboratory conditions a selective electrical gas discharge, similar to the natural occurring electrical plasma phenomena (lightning) and electrostatic discharge on the surface of biological and organic objects, as well as inorganic samples of different nature including water drops (Skarja *et al.*, 1988). Over the past decade, using the energy of the electric field in laboratory conditions from inorganic substances has been synthesized a variety of organic compounds - amino acids, proteins, nucleosides (Ignatov & Mosin, 2013). In these experiments (S. Miller's experiments, USA) were simulated the non-equilibrium processes with different sources of energy occurring in primary anoxic atmosphere in which was possible the synthesis of organic molecules from inorganic ones due to the energy of spark electrical discharges (electrosynthesis), short-wave UV radiation from the Sun and other sources of geothermal energy (Lazcano & Bada, 2004).

The aim of this research was to explore the possibility of coronal gas discharge effect in modeling non-equilibrium conditions with gas electric discharge simulating electrical processes going on in primary atmosphere and forecasting possible electrochemical reactions occurring in water via the treatment by the electric field of high intensity and frequency.

2. Material and Methods

2.1. Objects For Study

By using the method of coronal gas discharge spectral analysis with a combination of IR spectroscopy and the methods of nonequilibrium energy spectral analysis (NES) and differential non-equilibrium energy spectral analysis (DNES) were analyzed water samples of different origin derived from various Bulgarian

sources, as well as cactus juice and Mediterranean jellyfish *Cotylorhiza tuberculata* obtained from Aegean Sea (Chalkida, Greece). Before measurements the jellyfish was kept in seawater for two days.

2.2. Non-Equilibrium Gas Discharge Experiments

Experiments were carried out by using selective high-frequency electric discharge (SHFED) on a device with the electrode made of polyethylene terephthalate (PET, hostafan) with an electric voltage on the electrode 15 kV, electric impulse duration 10 μ s, and electric current frequency 15 kHz. The electrode of the device was made of hostafan, and was filled up with electro-conductive fluid. The spectral range of the emission was in the range $\lambda = 380\text{--}495$ nm and $\lambda = 570\text{--}750 \pm 5$ nm. The measurements were measured in electronvolts (eV). Detection of gas discharge glowing was conducted in a dark room equipped with a red filter. On the electrode put a photosensitive paper or color film. The object under study (human thumb) was placed on top of a sheet of photo paper or color film. Between the object and the electrode were generated impulses of the electric voltage 15 kV and electric frequency – 15–24 kHz; on the reverse side of the electrode was applied the transparent electrically conductive thin copper coating. Under these conditions in the thin contact gas space between the studied object and electrode was generated gas electric discharge in the form of characteristic glow around the object – a corona gas electric discharge in the range of $\lambda = 280\text{--}760$ nm, illuminates a color photo or a photographic film on which was judged about the bioelectric properties of the studied object. Along with the visible range, for this method were obtained color spectra in UV and IR range. Evaluation of the characteristic parameters of snapshots was based on the analysis of images treated by standard software package.

2.3. NES and DNES Spectral Analysis

The research was made with the method of non-equilibrium spectrum (NES) and differential non-equilibrium spectrum (DNES). The device measured the angles of evaporation of water drops from 72° to 0° . As the main estimation criterion was used the average energy ($\Delta E_{H...O}$) of hydrogen O...H-bonds between H_2O molecules in water samples. The spectrum of water was measured in the range of energy of hydrogen bonds at 0.08–0.1387 eV or $\lambda = 8.9\text{--}13.8$ μ m with using a specially designed computer program.

2.4. IR-Spectroscopy

IR-spectra of water samples were recorded on IR spectrometer Brucker Vertex (“Brucker”, Germany) (wavelength range: mid IR – $370\text{--}7800$ cm^{-1} ; visible – $2500\text{--}8000$ cm^{-1} ; resolution - 0.5 cm^{-1} , the accuracy of the wave number - 0.1 cm^{-1} at $\lambda = 2000$ cm^{-1}) and Thermo Nicolet Avatar 360 Fourier-transform IR (“Thermo Nicolet”, France).

2.5. Statistical Processing of the Experimental Data

Evaluation of the characteristic parameters was carried out on the basis of the analysis of the images processed by a standard software package. Statistical processing of the experimental data was performed using the statistical package STATISTISA 6 using a Student's *t*-criterion (at $p < 0.05$).

3. Results and Discussion

3.1. Visualisation Technique of GD-glowing

To visualize GD-glowing are used special electric devices generating electromagnetic field of high frequency and voltage (Pehek et al., 1976). Schematic diagram of a typical device is shown in Figure 1. The device contains the generator of electric field and an electrode made from PET or hostaphan. At the electrode is applied alternating electrical field with frequency of 15 kHz and voltage 15 kV (in other methods, these values are assumed to be equal 0.2–15 kHz and 5–30 kV). The studied object is grounded by a conductor, and placed on the electrode between which and the object is formed insulator, i.g. a thin layer of air which molecules undergo dissociation under the influence of the electromagnetic field generated by the electrode.

In this thin air layer with thickness of ~10–100 μm formed between the studied object and the electrode are developed the following processes (Ignatov & Tsvetkova, 2011):

- Excitation, polarization and ionization by the electric field of high electric voltage and frequency the main components of air – the molecules of nitrogen (78% N_2), oxygen (21% O_2) and carbon dioxide (0.046% CO_2). In the result of this is formed an ionized gas, i.e. gas with separated electrons having negative charges, creating a conductive medium, i.g. plasma;
- Formation of a weak electric current in the form of free moving electrons separated from molecules of N_2 , O_2 and CO_2 , which generate gas discharge between the studied object and the electrode. The form of gas discharge glowing, its density and surface brightness distribution is determined mainly by electromagnetic properties of the object;
- The transition of electrons from lower to higher energy levels and back again, during which there emanates a discrete quantum of light radiation in the form of photon emission. The transition energy of electrons depends on the external electric field and the electronic state of the material of the studied object. Therefore, in different areas surrounding the electric field, the electrons receive different energy impulses, i.e. “skipping” at different energy levels that results in emission of light photons with different wavelengths (frequencies) and the energy, coloring the contour of the glow in various spectral colors.

Processes outlined above form the gas discharge effect, allowing to study the electrical properties of the object at its interaction with an external electromagnetic field (Marinov & Ignatov, 2008). It was demonstrated that electrical conductivity of the object – the reciprocal of electrical resistance, expressed in siemens, has virtually no effect on the formation of GD-glow which depends mostly on the dielectric constant (Pehek *et al.*, 1976).

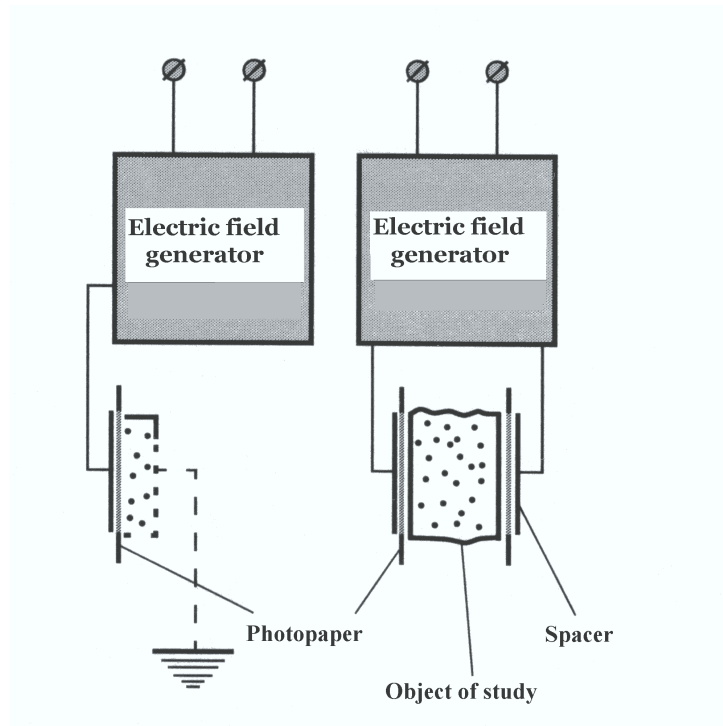


Figure 1. Schematic diagram of the device for visualizing of GD-glow

Dependence of the electrical conductivity σ ($\text{Ohm}^{-1} \cdot \text{m}^{-1}$) and the thermal conductivity K ($\text{W/m} \cdot \text{K}$) is determined by the Wiedemann-Franz law:

$$\frac{K}{\sigma} = \frac{\pi^2}{3} \left(\frac{k}{e} \right)^2 T, \quad (1)$$

where k – Boltzmann constant ($1.380662 \cdot 10^{-23}$ J/K), e – electron charge ($-1.02176 \cdot 10^{-19}$ Kl), T – temperature (K).

For the calculation of the basic physical parameters of the gas discharge is used the experimental dependence of the conductivity per unit area of the recording medium on the following parameters of the electric discharge:

$$\sigma = a - \left[U_p \frac{(d_2 + \delta)}{\delta \cdot d_2} \varepsilon_0 \frac{(d_2 + \delta)}{\delta \cdot d_2} \right], \quad (2)$$

where: $\delta = \frac{d_1}{\varepsilon_1} + \frac{d_3}{\varepsilon_3};$

a – slope rate of electrical impulse;

T – duration of the electrical impulse;

U_p – breakdown voltage of the air layer gap between the subject and the recording medium;

d_1 – width of the object;
 d_2 – width of the zone of action of the electric field;
 d_3 – width of the recording medium;
 ϵ_0 – dielectric permittivity of the air ($\epsilon_0 = 1.00057$ F/m);
 ϵ_1 – dielectric permittivity of the studied object;
 ϵ_3 – dielectric permittivity of the recording medium.

To calculate the breakdown voltage of the air layer is used this formula:

$$U_p = 312 + 6,2d_2 \quad (3)$$

As a result of mathematical transformations is obtained a quadratic equation describing the width of the air gap layer:

$$6,2d_2^2 + (aT - 6,2\delta - 312)d_2 + 312\delta = 0, \quad (4)$$

Which is reduced to the standard quadratic equation:

$$ax^2 + bx + c = 0, \quad (5)$$

where $a = 6.2$;

$$b = aT - 6,2\delta - 312;$$

$$c = 312\delta$$

This equation has two solutions:

$$x_{1,2} = \frac{-b \pm \sqrt{b^2 - 4ac}}{2a} \quad (6)$$

Correspondingly:

$$d_{1,2} = \frac{-[a \cdot T - 6,2\delta - 312] \pm \sqrt{[a \cdot T - 6,2\delta - 312]^2 - 77,376\delta}}{12,4}, \quad (7)$$

The above equations allow to calculate the maximum and the minimum width of the air gap layer for the occurrence of the electric discharge with which help is being formed the electrical image of the studied object, which spectrum is shown in Figure 2 depending on the energy of the emitted light photons. Other gas discharge characteristics for various objects vary in character and light intensity, size of contour glow and color spectrum and depend both on its own electromagnetic radiation and the dielectric constant of the object. The intensity depends on the electric voltage applied on the electrode.

**Energy of the Separated Photons of Color
Coronal (Kirlian) Glow Ignatov, 2007**

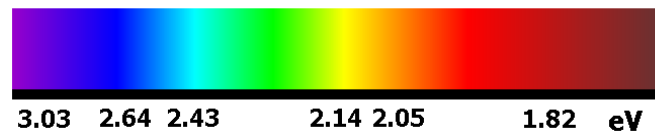


Figure 2. Spectrum of coronal gas discharge spectral analysis and the energy of the emitted photons (eV) (I. Ignatov, 2007)

As showed by the experiments (Ignatov & Mosin, 2012), the characteristics of GD-glow of different biological objects vary in characteristics and intensity of light, size and color, and depend both on its own electromagnetic radiation and the dielectric constant of the object's material. GD-glowing intensity depends on the electric voltage of an electric current applied to the electrode. At low values of the electric voltage GD-emission does not occur, and at too high voltage there is a threat of dielectric breakdown, which is highly undesirable in experimental studies. Small electric current frequency can also cause dielectric breakdown. The optimum lower limit frequency of the electric current in this method is taken to be equal to 500 Hz, depending on the electrical potential difference between the electrode and the dielectric. Thus, for a standard glass electrode (glass as a dielectric) is possible with low voltage electrical current to obtain the characteristic GD-glowing at the lower limit of the electric frequency at ~200 Hz. The upper frequency limit for the electric current lies between ~15 kHz and ~20 kHz, and mainly depends on the electrical parameters of the electrode material. Between the lower and upper bound are observed two characteristic intense peaks: at ~650 Hz and at ~7000 Hz. In the first case, at a low frequency of the electric current plays an important role permittivity. In the second case – at a high frequency of electric current, the electrical conductivity of the object is not important, but more important is the object's own electromagnetic field, which is not uniform, and is not in direct relation with the electrical conductivity. As an electrode may be used a plate made of a rigid polymeric material (epoxy, PET hostafan, polyester) coated on one side with a thin electrically conductive copper layer. In this case the function of a dielectric performs the polymer material. In order to avoid the dielectric breakdown at the edges of the dielectric, the layer of copper at ~10 mm from the edge of the electrode is removed. The electrode treated in this way is suitable for use with high voltage electrical current.

The process of photographing objects is carried out in a dark room or at a red light filter. On the dielectric plate, serving as an electrode creating the electric field of high voltage, is placed a sheet of light sensitive paper or a film. The object under study (water droplets) is placed on the top of the film. Between the studied object and the dielectric plate is applied the pulsating electric voltage from the electromagnetic field

generator. At the electric field with high voltage and frequency in the air gap zone of the contact between the object and the plate there develops gas electrical discharge (avalanche or slide) characterized by GD-glow around the object - corona electrical discharge at the wavelength $\lambda = 380-490$ nm and $\lambda = 560-780$ nm, illuminates the photo paper or the film. After developing photographic paper most striking areas become darker, this is typical for any photographic process. Since the investigated object is in contact with the photo paper (in the form of a circle in the center), this area is not illuminated.

In Bulgarian Scientific Research Center of Medical Biophysics to visualize the GD-glowing is developed the method of the selective high frequency electric discharge (SHFED) performed with using the electrode of a polymer material hostafan characterized by high dielectric strength (160-200 kV/mm). Photographing of GD-glow in this methodology is one of the physical methods, in which the image quality when using the film is higher than using the “Polaroid” camera or digital computer methods. The electrical voltage applied to the electrode of the device makes up ~15 kV at a frequency of electric current at ~15 kHz. This makes it easy to obtain and carry out the parametric analysis of GD-image. This method in combination with IR spectrometry, NES-, and DNES-methods was used in the modeling non-equilibrium conditions with gas electric discharge simulating primary atmosphere.

3.2. Modeling of Non-equilibrium Conditions with Gas Electric Discharge

The first experiments on the modeling of non-equilibrium conditions with gas electric discharge simulating primary atmosphere and electrosynthesis of organic substances by the energy of the electric field in a primary oxygen-free atmosphere, were held in 1953 by S. Miller (USA) (Miller, 1953). For this aim the mixture of water and gases consisted of hydrogen (H_2), methane (CH_4), ammonia (NH_3) and carbon monoxide (CO) was placed into a closed glass container being exposed by pulsating electrical spark discharges at the temperature of boiling water; oxygen was not allowed into the unit. After processing the reaction mixture by the electric discharge it was found that from the initial inorganic substance was synthesized organic compounds - aldehydes and amino acids. Experiments found that approximately ~10-15% of carbon was transferred into an organic form. However, about ~2% of carbon was detected in the amino acids, the most common of which was glycine. Initial analysis showed the presence in the reaction mixture obtained after the processing by spark electric discharge 5 amino acids. A more complete analysis carried out in 2008 (Johnson *et al.*, 2008), showed the formation by electrosynthesis in the reaction mixture 22 amino acids having from 5 to 20 carbon atoms in the molecule (Figure 3). Interestingly is that along with the amino acids in the reaction mixture after the treatment with electric spark discharges were detected trace amounts of nucleic acid precursors - nucleosides.

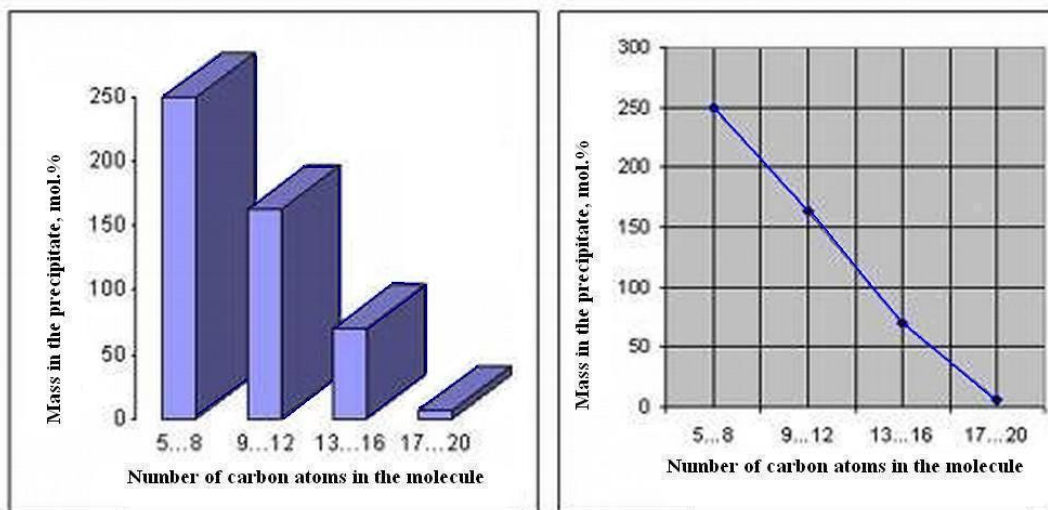


Figure 3. Distribution of carbon compounds obtained in the experiments of S. Miller, mass and number of carbon atoms in the molecule (diagrams constructed by the authors according to the S. Miller experiments)

S. Miller's experiments were reproduced in different variations with a combination of electrical discharges, UV-radiation and heat. Thus, in aqueous solutions of formaldehyde (CH_2O) with hydroxylamine (NH_2OH), formaldehyde with hydrazine (N_2H_4) and HCN, after heating a reactionary mixture to $+95\text{ }^\circ\text{C}$ were detected amino acids (Harada & Fox, 1964). In model experiments reaction products were polymerized into short peptide chains that is the important stage towards inorganic synthesis of protein. In a reactionary mixture of water with 4-aminoimidazole-5-carboxamide, 4-aminoimidazole-5-carboxamide, NH_3 , formamidine and urea at heating to $+95\text{ }^\circ\text{C}$ were synthesized purines (Figure 4). In 1960 A Wilson (Wilson, 1960) after processing by electric spark discharge water vapor, ammonia (NH_3), hydrogen sulfide (H_2S), sulfur and yeast ash, obtained in the reaction mixture the larger organic polymer molecules containing 20 or more carbon atoms. These polymers in aqueous solutions formed thin films with surface area of $\sim 1\text{ cm}^2$, resembling surfactants concentrated on the surface of the air-water interface (Figure 5). It is assumed that these films of polymer molecules were synthesized at the boundary between different phases, and played an important role in the early stages of the evolution of the first membrane-organized microstructures - the proteinoid microspheres (Nakashima, 1987) formed from thermal proteinoids at thermal treatment of the reaction mixture at temperatures of $+95\text{ }^\circ\text{C}$. Thermal proteinoids are short protein-like molecules resembling early evolutionary forms of proteins. They are formed from amino acid mixtures subjected to influence of temperatures from $+60\text{ }^\circ\text{C}$ up to $+170\text{ }^\circ\text{C}$, and consisted of 18 amino acids usually occurring in protein hydrolyzates. The synthesized proteinoids are similar to natural proteins on a number of other important properties, e.g. on linkage by nucleobases and ability to cause the reactions similar to those catalyzed by enzymes in living organisms as decarboxylation, amination, deamination, and oxidoreduction. Proteinoids are capable to catalytically decompose glucose (Fox & Krampitz, 1964) and to have an effect similar to the action of α -melanocyte-stimulating hormone (Fox & Wang, 1968). The best results on polycondensation were achieved with the mixes of amino acids containing aspartic and glutamic acids, which are essential

amino acids occurring in all modern living organisms. By morphological features the proteinoid microspheres with a diameter $\sim 5\text{--}10\ \mu\text{m}$ resemble cell membrane, which in certain conditions (increased pH) may be double (Figure 6). The catalyst for their formation could serve sulfur and its derivatives which were found in ancient rocks in the form of grains of sulfides, as well as pyrite sands. Synthesis of proteinoid microspheres from a mixture of thermal proteinoids is important because it provides material for the next stage of the evolution of life. This is the stage from disparate organic molecules to organized proteinoid molecules having organized structure and separated from the surrounding environment by primitive membrane.

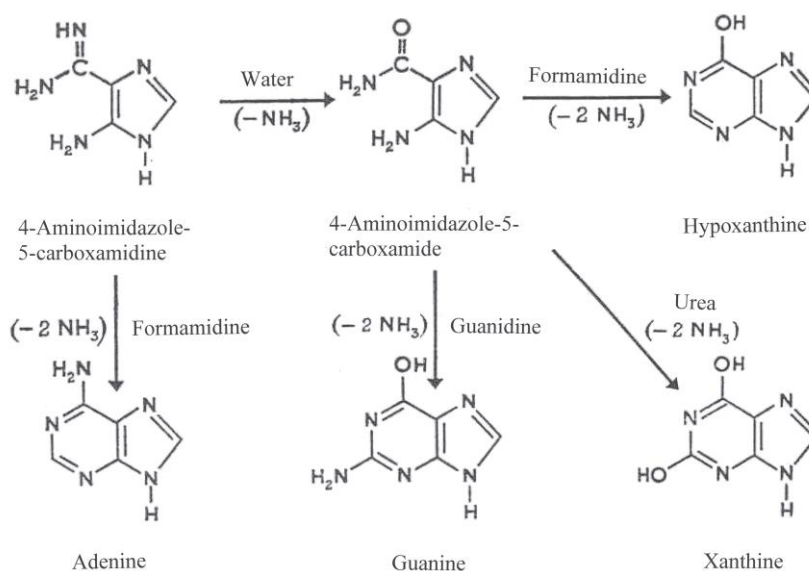


Figure 4. Prospective mechanisms of thermal ($+95\ ^\circ\text{C}$) synthesis of purines - hypoxanthine, adenine, guanine and xanthine in aqueous solutions from their predecessors - 4-aminoimidazole-5-carboxamide, 4-aminoimidazole-5-carboxamide, water, NH_3 , formamide and urea

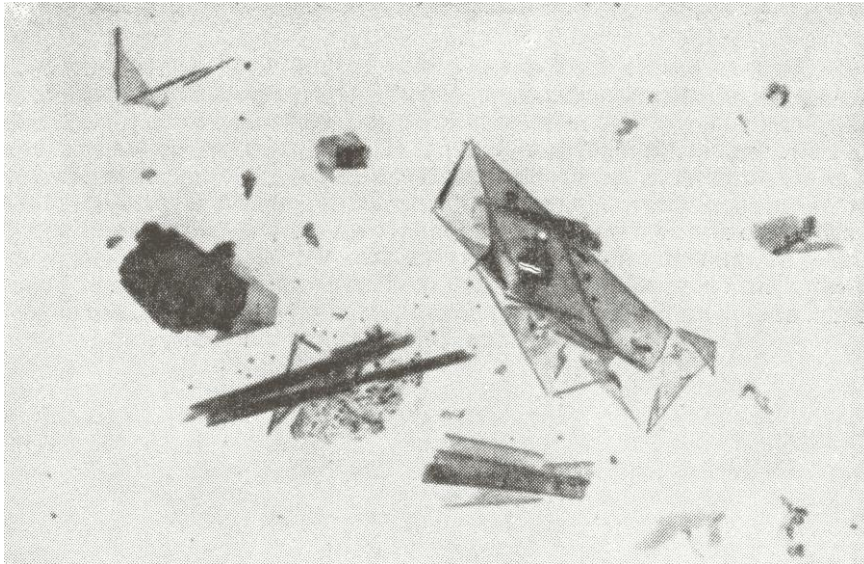


Figure 5. Thin films of organic polymers formed by the electrical spark discharges in a mixture of H_2O , NH_3 , H_2S , sulfur and yeast ash (Wilson, 1960)

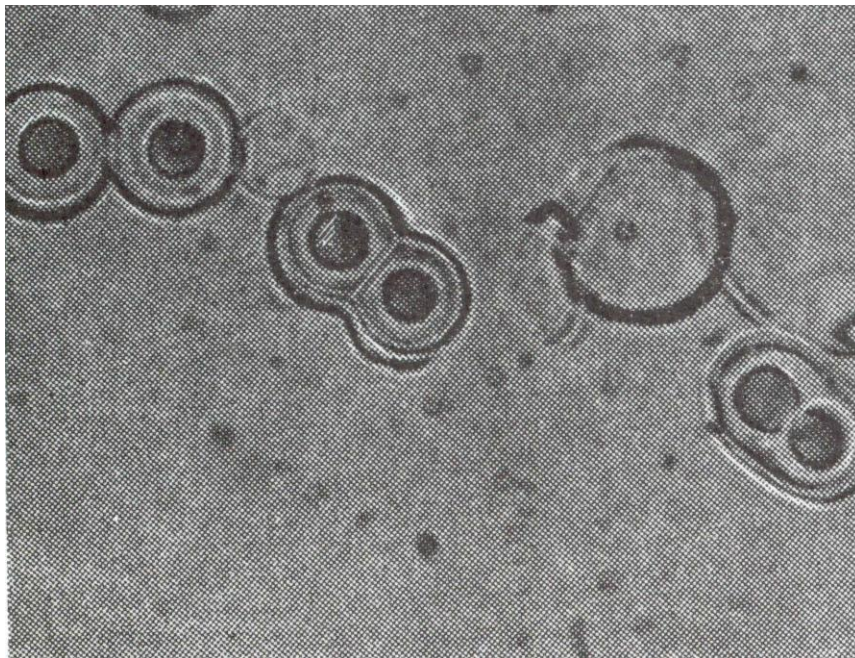


Figure 6. Electron micrographs of sections of proteinoid microspheres in scanning electron microscope (magnification $\times \sim 1000$ times) (Nakashima, 1987).

It should be noted that in the implementation of the gas discharge effect as well as in experiments of S. Miller are modeled extreme non-equilibrium conditions with gas electric discharge, resulting that in a thin

layer of air gap with thickness $\sim 100 \mu\text{m}$ are formed reactive radicals reacting with each other to form new compounds (electrosynthesis). Such extreme conditions are thought to have occurred in the primary oxygen-free atmosphere of the Earth, which supposedly consisted of a mixture of water and gases – H_2 , CH_4 , NH_3 and CO , subjected to spark electrical discharges (lightning) under the conditions of high solar (UV) and geothermal activity.

According to our previous experiments, the first living structures may have evolved in warm and hot mineral water with a high content of bicarbonate (HCO_3^-) anions, cations of alkali metals (Na^+ , Ca^{2+} , Mg^{2+} , etc.) and deuterium in the form of HDO (Ignatov & Mosin, 2013a). Similar composition and water temperature were modeled on the electrode of the gas discharge device made of hostafan, with electric voltage - 15 kV, electric impulse duration - 10 μs ; electric current frequency - 15 kHz, wherein the air gap layer on the boundary with water sample was formed corona electrical discharge, similar to plasma phenomena (lightning) and electrostatic discharge on the surface of organic and inorganic samples of various kinds. Investigated water sample before being placed onto the electrode was heated to boiling temperature and then cooled. In preliminary experiments in the interelectrode space was formed a semblance of an organized structure with dimensions $\sim 1.2\text{-}1.4 \text{ mm}$ (Figure 7). In the control sample of water on the electrode the structure was not organized. With increasing the length of the gas electric discharge, the structure was somewhat increased in size. Moreover, in experiments was observed formation of small structures and their further “adjoining” to the larger structure. This experiment shows that, under certain external conditions (corona electrical discharge, heat) it is possible the structural organization of water. It should be noted that water in natural conditions was heated by the magma. The structure formed from the thermoheated water was evidently a result of self-organization. Living organisms are complex self-organizing systems. Thermodynamically they belong to the open systems because they are constantly exchanging substances and energy with the environment. The changes in the open systems are relatively stable in time. The stable correlation between components in thermodynamic open system is called a dissipative structure. According to I. Prigozhin, the formation of dissipative structures and the elaboration to living cells is related to changes in entropy (Nikolis & Prigozhin, 1979). Taking these results into consideration, it is possible to conclude that the initial stage of evolution, apparently, was connected with formation at high temperature the mixtures of amino acids and nitrogenous substances – analogues of nucleic acids. Such synthesis is possible in aqueous solutions under thermal conditions in the presence of H_3PO_4 as a catalyst. The next stage is polycondensation of amino acids into thermal proteinoids at temperatures $65\text{-}95 \text{ }^\circ\text{C}$. After that in a mix of proteinoids in hot water solutions are formed membrane like structures – proteinoid microspheres. In 2011 T. Sugawara (Japan) created membrane like proto cells from aqueous solution of organic molecules, DNA and synthetic enzymes under temperature close to water’s boiling point $+95 \text{ }^\circ\text{C}$ (Sugawara, 2011). These experiments are excellent confirmation of the possibility that life and living matter originated in hot water.



Figure 7. An organized structure in water sample subjected to temperatures up to 100 °C in the electric field of high voltage and and frequency. The material of the electrode – hostafan; electric voltage - 15 kV, electric impulse duration 10 μs; electric current frequency 15 kHz.

3.3. Study of GD-glowing of Water in Electric Field of High Voltage and Frequency

The exposure high-frequency electric discharge to water appears in the form of characteristic GD-glowing around water drops. From the physical point of view, this process is characterized by a process of non-equilibrium transport of electric discharge in adjacent to the object of study thin air gap being ionized by the electric field. The authors believe that the emergence of GD-glow around water drops may be explained by taking into account the energy of the electric field and the change due to the influence of the electric field on the water structure, which in turn may be due to intermolecular rearrangements within associative elements of water. This fact may indicate that the structural elements of water may possess “information” properties.

The authors consider that it seems unlikely that life originated in the “chaotic” non-informative water. Living organisms and water are complex, self-organizing systems having a characteristic structure. According to recent data, water is an associated liquid consisting of associated elements - clusters with general formula $(\text{H}_2\text{O})_n$, where $n = 3-50$ (Ignatov & Mosin, 2013b). These associates can be described as unstable groups (dimers, trimers, tetramers, pentamers, hexamers etc.) in which individual H_2O molecules are linked by van der Waals forces, dipole-dipole and other interactions with charge transfer, including hydrogen $\text{H}\dots\text{O}$ bonding (Ignatov & Mosin, 2013c). At room temperature, the degree of association of H_2O molecules may vary from 2 to 21.

The hydrogen bond results from interaction between electron-deficient H-atom of one H_2O molecule (hydrogen donor) and unshared electron pair of an electronegative O-atom (hydrogen acceptor) on the neighboring H_2O molecule; the structure of hydrogen bonding, therefore may be defined as $\text{O}\dots\text{H}^{\delta+}-\text{O}^{\delta-}$. As the result, the electron of the H-atom due to its relatively weak bond with the proton easily shifts to the electronegative O-atom. The O-atom with increased electron density becomes partly negatively charged – δ^- ,

while the H-atom on the opposite side of the molecule becomes positively charged – δ^+ that leads to the polarization of $O^- - H^+$ covalent bond. In this process the proton becomes almost bared, and due to the electrostatic attraction forces are provided good conditions for convergence of $O \dots O$ or $O \dots H$ atoms, leading to the chemical exchange of a proton in the reaction $O-H \dots O \leftrightarrow O \dots H-O$. Although this interaction is essentially compensated by mutual repulsion of the molecules' nuclei and electrons, the effect of the electrostatic forces and donor-acceptor interactions for H_2O molecule compiles 5–10 kcal per 1 mole of substance. It is explained by negligible small atomic radius of hydrogen and shortage of inner electron shells, which enables the neighboring H_2O molecule to approach the hydrogen atom of another molecule at very close distance without experiencing any strong electrostatic repulsion. In respect of energy hydrogen bond has an intermediate position between covalent bonds and intermolecular van der Waals forces, based on dipole-dipole interactions, holding the neutral molecules together in gasses or liquefied or solidified gasses. Hydrogen bonding produces interatomic distances shorter than the sum of van der Waals radii, and usually involves a limited number of interaction partners. These characteristics become more substantial when acceptors bind H-atoms from more electronegative donors. Hydrogen bonds hold H_2O molecules on 15% closer than if water were a simple liquid with van der Waals interactions. The hydrogen bond energy compiles 5–10 kcal/mole, while the energy of $O-H$ covalent bonds in H_2O molecule – 109 kcal/mole (Arunan *et al.*, 2011). The values of the average energy ($\Delta E_{H \dots O}$) of hydrogen $H \dots O$ -bonds between H_2O molecules make up 0.1067 ± 0.0011 eV (Antonov & Galabova, 1992). With fluctuations of water temperature the average energy of hydrogen $H \dots O$ -bonds in water associates changes. Therefore, the hydrogen bonds in the liquid state are relatively weak and unstable: they can easily occur and collapse as a result of thermal fluctuations (Ignatov & Mosin, 2013a). This process leads to structural inhomogeneity of water characterizing it as an associated heterogeneous two-phase liquid with short-range ordering, i.e. with regularity in mutual positioning of atoms and molecules, which reoccurs only at distances comparable to distances between initial atoms, i.e. the first H_2O layer. Changing the position of one structural element (H_2O molecules) under the influence of any external factor, or changing the orientation of the neighboring H_2O molecules ensures high sensitivity of the structural elements of water to various external influences (electromagnetic, thermal, sound fields, etc.).

Water molecules in the liquid state at standard conditions (1 atm. 22 °C) are able to perform oscillating movements about its axis of rotation, as well as random and directed movement, whereby individual molecules can be moved from one location to another through the volume of water via cooperative interactions. As a result, in aqueous solutions is possible autoprotoliz i.e. take off a proton H^+ from one molecule of water, followed by moving and adding H^+ to a neighboring molecule H_2O , leading to delocalization of a proton within a cluster to form a hydronium ion as H_3O^+ , $H_5O_2^+$, $H_7O_3^+$, $H_9O_4^+$, etc. Hydrogen bonding leads to the formation of the next hydrogen bond and redistribution of electrons, which in its turn promotes the formation of the following hydrogen bond, which length increasing with distance. Cooperative hydrogen bonding increases the $O-H$ bond length, at the same time causing a reduction in the $H \dots O$ and $O \dots O$ distances (Goryainov, 2012). The protons held by individual H_2O molecules may switch partners in an ordered manner within hydrogen networks (Bartha *et al.*, 2003). This property explains the extremely labile, mobile character of interaction of water associates with each other. In the mathematical model of water it is assumed that water consists of a variety of association elements - neutral clusters $(H_2O)_n$ and charged cluster ions $[(H^+)(H_2O)_n]^+$ and

$[(OH)(H_2O)_n]^-$ with different types of similarity which can form quasicrystalline structure, wherein n in mathematical calculations can reach tens or even hundreds of units (Ignatov & Mosin, 2013a; Ignatov & Mosin, 2013b). This property explains the extremely labile, mobile character of the electrostatic interaction of associative elements of water with each other, due to which occurs the construction of structural elements of water into hollow cells (clathrates) up to 0.5-1.0 μm .

Due to the fact that H_2O molecules are polar dipoles, they are thought to have oriented in the electric field. In the study of GD-glowing of water droplets it was proposed that electric glow was partly due to the polarity of H_2O molecules and their orientation by an external electric field (Ignatov & Mosin, 2013e). Polarization is a physical phenomenon associated with electromagnetic waves, when the electromagnetic field oscillates (fluctuates) in one particular plane perpendicular to the direction of wave propagation. Water has the highest dielectric constant and it determines its chemical properties as an universal solvent. GD-images of water drops of various origin and degree of purification indicate that the different water samples interact in different ways with the electric field. Moreover water is a source of super-weak and weak alternating electromagnetic radiation. In this case, it is possible the induction of the corresponding electromagnetic field and resonance effects of combination (superposition) of electromagnetic fields capable to altering the structural and functional characteristics of biological objects by 70-80% consisting of water. As it was demonstrated by I. Ignatov (Figure 8), the character of GD-glowing of water drops placed in an alternating electric field of high voltage and frequency influences the origin of water sample, the method of the water treatment, the presence of impurities in water and other factors.

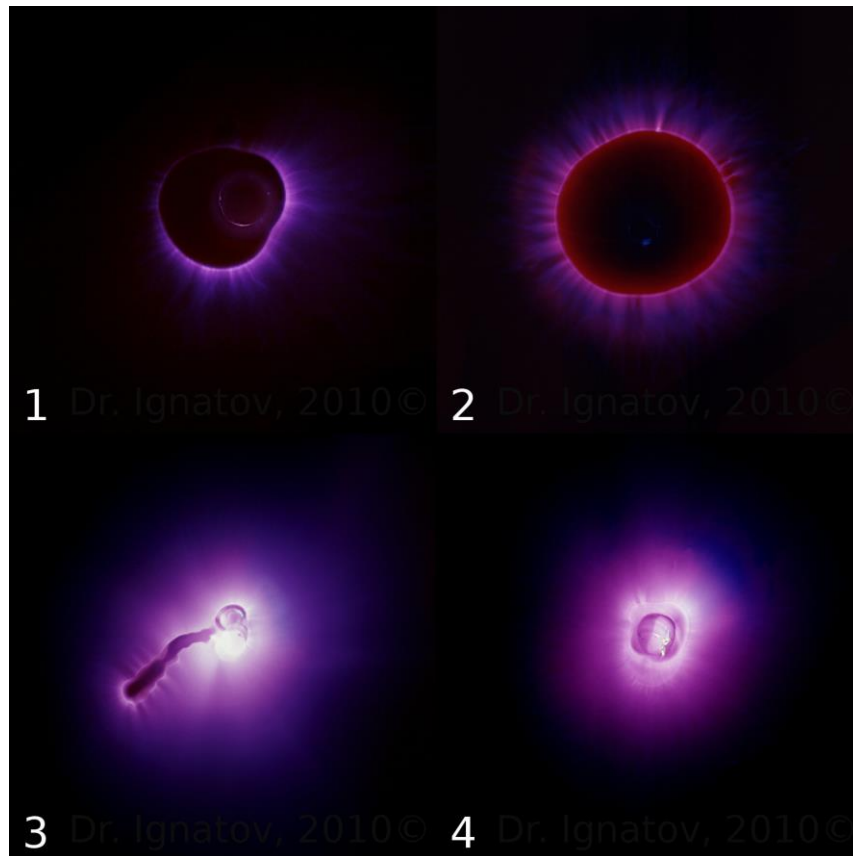


Figure 8. Color gas discharge spectral analysis of water droplets of different origin (I. Ignatov, 2012) (the electrode voltage - 15 kV, electric current frequency - 15 kHz): 1 - tap water; 2 - mountain water (Teteven, Bulgaria); 3 - seawater (Hammamet, Tunisia); 4 - Karst and mineral water (Zlatna Panega, Bulgaria)

3.4. IR, NES and DNES Spectral Analysis of Water

Experiments with a non-equilibrium electric discharge in aqueous solutions in combination with the method of IR spectroscopy allow to prognose the conditions under which the first organic forms evolved (Ignatov & Tsvetkova, 2011; Ignatov, 2012; Ignatov & Mosin, 2013c; Ignatov & Mosin, 2013d). Experiments have shown that the most favorable for the maintenance of biochemical reactions are karst mineral waters interacting with CaCO_3 , and then seawater (Ignatov, 2010; Ignatov & Mosin, 2013e; Ignatov & Mosin, 2013f; Ignatov & Mosin, 2013g). Circulating in the cavities, microcracks and channels waters from karst springs became enriched with $\text{Ca}(\text{HCO}_3)_2$, actively interacting with the organic matter, and may contain other dissolved in water ions (Zn^{2+} , Mg^{2+} , Fe^{2+} , Fe^{3+} , SO_4^{2-}), which can act as catalysts for biochemical reactions (Mulkidjanian & Galperin, 2009). Self-organization of primary organic forms in aqueous solutions, was probably supported by geothermal energy sources, electric spark discharges and solar radiation.

In further studies was used the effect, established experimentally by A. Antonov and L. Yuskesseliava (Antonov & Yuskesseliava, 1983) that at the process of evaporation of water drops, the wetting angle θ

decreases discreetly to 0, while the diameter of water drop basis is only slightly altered. Based on this effect, by means of measurement of the wetting angle within equal intervals of time is determined the function of distribution of H₂O molecules according to the value of f(θ). The distribution function is denoted as the energy spectrum of the water state. A theoretical research established the dependence between the surface tension of water and the energy of hydrogen bonds among individual H₂O-molecules (Antonov, 1995). The hydrogen bonding results from interaction between electron-deficient H-atom of one H₂O molecule (hydrogen donor) and unshared electron pair of an electronegative O-atom (hydrogen acceptor) on the neighboring H₂O molecule; the structure of hydrogen bonding may be defined as O^{δ+} ••• H^{δ-} O^{δ-}.

For calculation of the function f(E) represented the energy spectrum of water, the experimental dependence between the wetting angle (θ) and the energy of hydrogen bonds (E) is established:

$$f(E) = \frac{14,33f(\theta)}{[1-(1+bE)^2]^2}, \quad (8)$$

where b = 14.33 eV⁻¹

The relation between the wetting angle (θ) and the energy (E) of the hydrogen bonds between H₂O molecules is calculated by the formula:

$$\theta = \arcsin(-1 - 14.33E) \quad (9)$$

The energy spectrum of water is characterized by a non-equilibrium process of water droplets evaporation, therefore, the term non-equilibrium spectrum (NES) of water is used. The energy of hydrogen bonds measured by NES is determined as $\bar{E} = -0.1067 \pm 0.0011$ eV.

The difference $\Delta f(E) = f(\text{samples of water}) - f(\text{control sample of water})$

– is called the “differential non-equilibrium energy spectrum of water” (DNES).

Thus, DNES spectrum may serve as an indicator of structural changes of water as a result of various external factors. We have carried out the research of various samples of mineral water from mineral springs and seawater from Bulgaria by using IR-spectroscopy and DNES-method (Figure 9, curves 1–5). For this aim we employed the DNES method that shows the average energy of hydrogen bonds between individual molecules of H₂O and the function of the distribution of energies Δf between individual H₂O molecules (Table), relative to the control – deionized water. Cactus juice was also investigated by the DNES method (Figure 9, curve 1). Cactus was selected as a model system because this plant contains approximately 90% of water. The closest to the DNES-spectrum of cactus juice was the DNES-spectrum of mineral water contacting with Ca²⁺ and HCO₃⁻ ions (Figure 9, curve 2). DNES-spectra of cactus juice and mineral water have magnitudes of local energetical maximums at –0.1112; –0.1187; –0.1262; –0.1287 and –0.1387 eV. Similar local maximums in the DNES-spectrum between cactus juice and seawater were detected at –0,1362 eV. The DNES-spectrum of the control sample of deionized water (Figure 9, curve 5) was substantially different from the DNES-spectra of seawater and mineral water.

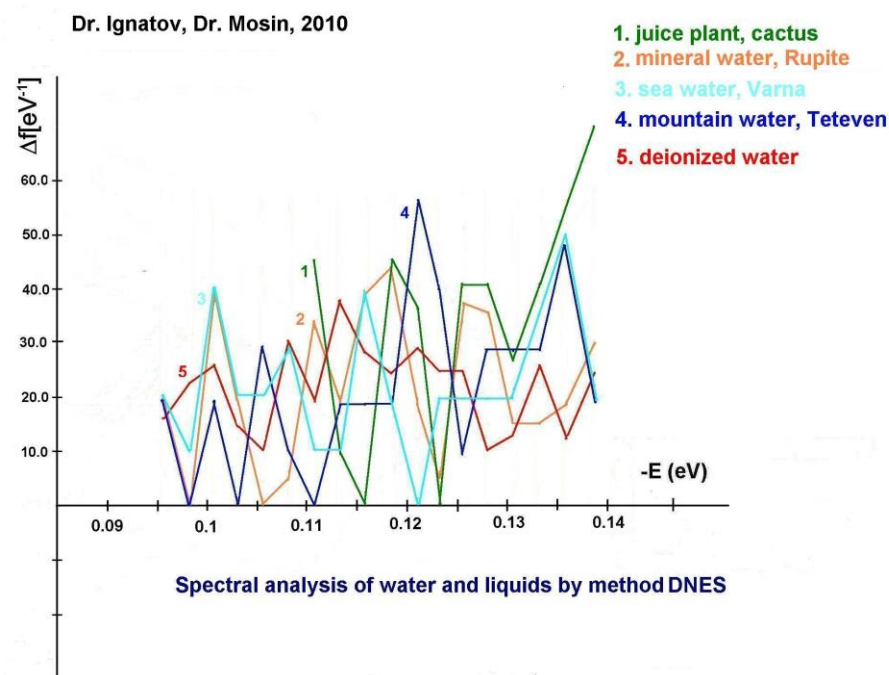


Figure 9. DNES-spectra of water samples of various origin: 1 – cactus juice; 2 – mineral water from Rupite village (Bulgaria); 3 – seawater (Varna, Bulgaria); 4 – mountain water (Teteven, Bulgaria); 5 – deionized water (the control)

As shown from these data, the closest to the spectrum of cactus juice was mineral water from Rupite Village (Bulgaria), which DNES and IR spectrum is shown in Figure 9 and Figure 10 (Thermo Nicolet Avatar 360 Fourier-transform IR). IR-spectra of cactus juice and mineral water with HCO_3^- (1320–1488 mg/l), Ca^{2+} (29–36 mg/l), pH (6.85–7.19), have local maximums at $\lambda = 8.95; 9.67; 9.81; 10.47$ and $\lambda = 11.12 \mu m$ (Fourier-IR spectrometer Brucker Vertex). Common local maximums in the IR-spectrum between cactus juice and seawater are detected at $\lambda = 9.10 \mu m$. The local maximums obtained with IR method at $\lambda = 9.81 \mu m$ ($k = 1019 \text{ cm}^{-1}$) and $\lambda = 8.95 \mu m$ ($k = 1117 \text{ cm}^{-1}$) (Thermo Nicolet Avatar 360 Fourier-transform IR) are located on the spectral curve of the local maximum at $\lambda = 9.7 \mu m$ ($k = 1031 \text{ cm}^{-1}$) (Figure 3). With the DNES method were obtained the following results – $\lambda = 8.95; 9.10; 9.64; 9.83; 10.45$ and $11.15 \mu m$, or $k = 897; 957; 1017; 1037; 1099$ and 1117 cm^{-1} in wave numbers.

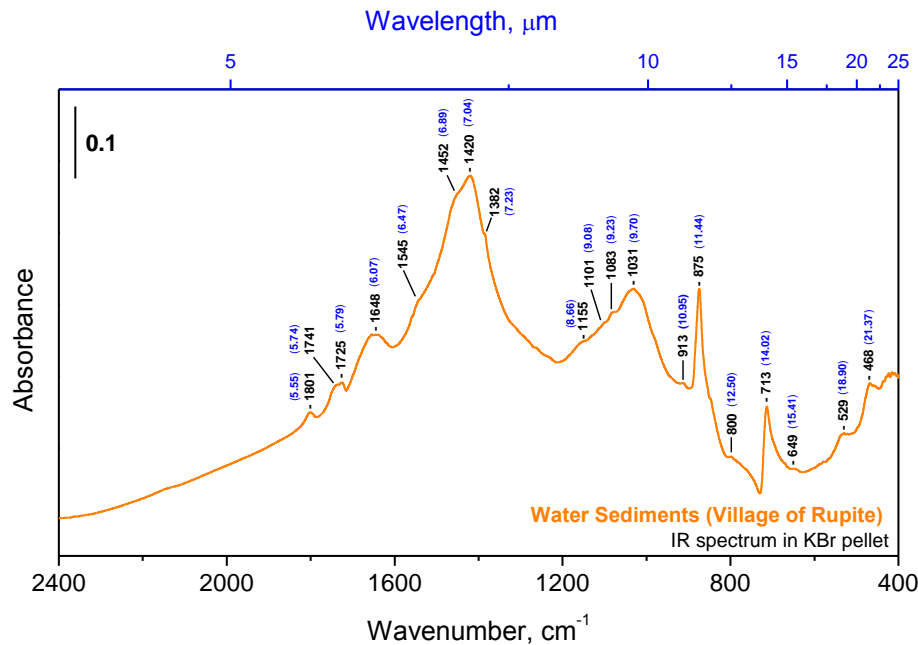


Figure 10. IR-spectrum of water obtained from Rupite Village (Bulgaria)

Table. Characteristics of spectra of water of various origin obtained by DNES-method*

-E, eV			λ , μm	k, cm^{-1}
Cactus juice	Mineral water from Rupite Village (Bulgaria)	Seawater		
0.1112	0.1112	–	11.15	897
0.1187	0.1187	–	10.45	957
0.1262	0.1262	–	9.83	1017
0.1287	0.1287	–	9.64	1037
0.1362	–	0.1362	9.10	1099
0.1387	0.1387	–	8.95	1117

The note:

*The function of the distribution of energies Δf between individual H_2O molecules was measured in reciprocal electron volts (eV^{-1}). It is shown at which values of the spectrum $-E$ (eV) are observed the biggest local maximums of this function; λ – wave length; κ – wave number.

The results with Mediterranean jellyfish *Cotylorhiza tuberculata* indicated that jellyfish has two main local maximums in IR-spectra at $\lambda = 8.98 \mu\text{m}$ and $\lambda = 10.18 \mu\text{m}$ (Figure 11). On comparison seawater has a local maximum at $\lambda = 8.93 \mu\text{m}$ in IR-spectra. These results were obtained with Thermo Nicolet Avatar 360

Fourier-transform IR. With DNES method the local maximums in spectra for jellyfish are at $\lambda = 8.95 \mu\text{m}$ and $\lambda = 10.21 \mu\text{m}$, and for seawater at $\lambda = 9.10 \mu\text{m}$. The differential spectrum was recorded for the jellyfish and seawater with using the Thermo Nicolet Avatar 360 Fourier-transform IR method. In the IR-spectrum of the jellyfish local maximums, detected by Thermo Nicolet Avatar 360 Fourier-transform IR and DNES method, are more pronouncedly expressed. Measurements demonstrate that two common local maximums are observed in IR-spectra of jellyfish and seawater. These maximums, however, are not observed in the IR-spectrum of cactus juice and the IR-spectrum of mineral water from Rupite (Bulgaria). The jellyfish body contains approximately 97% of water and is unstable while taken off from water. The explanation for this is the smaller concentration of salts in the jellyfish than in seawater and, therefore, the smaller number of local maximums in the IR-spectrum of jellyfish in relation to IR-spectrum of seawater.

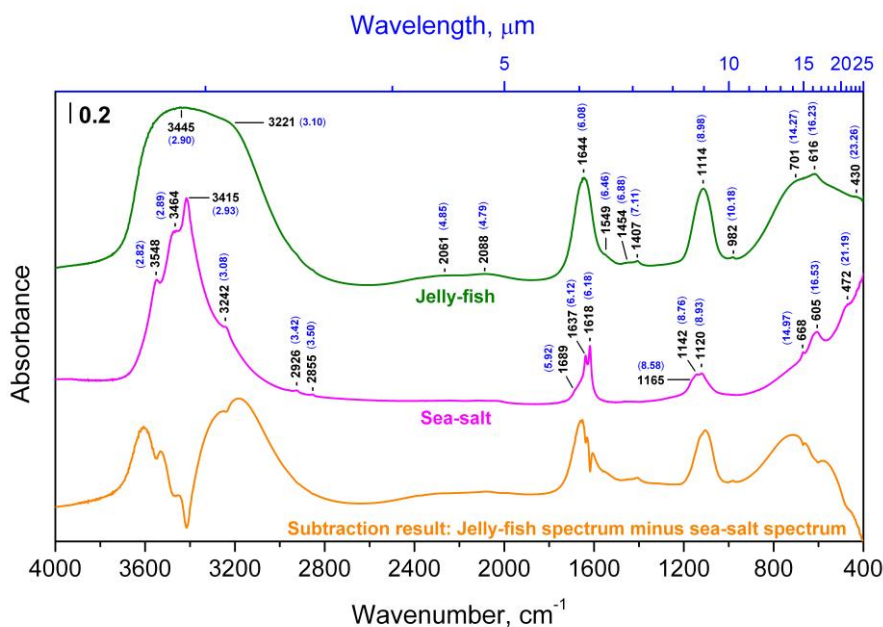


Figure 11. IR-spectra of seawater obtained from Varna (Bulgaria) and jellyfish *Cotylorhiza tuberculata*, Chalkida (Greece), Aegean Sea

Such a character of IR- and DNES-spectra and distribution of local maximums may prove that hot mineral alkaline water is preferable for maintenance of life compared to other types of water analyzed by these methods. Thus, in hot mineral waters the local maximums in the IR-spectrum are more manifested compared to the local maximums obtained in IR-spectrum of the same water at a lower temperature. The difference in the local maximums from +20 °C to +95 °C at each 5 °C according to Student *t*-criterion – $p < 0.05$.

Another important parameter was measured by the NES method – the average energy ($\Delta E_{H...O}$) of hydrogen H...O-bonds among individual H₂O molecules in the process of formation of cluster associates with

formula $(\text{H}_2\text{O})_n$ (dimer, trimer) constituting $-0,1067 \pm 0,0011$ eV, which coincides with the main peak in the NES spectrum of water (Figure 12). When the water temperature changes, the average energy of hydrogen H...O-bonds in water associates alternates. This testified about the restructuring of average energies among individual H_2O molecules with a statistically reliable increase of local maximums in DNES-spectra. Spectral analysis carried out by the DNES method on water samples indicates the orientation process (restructuring) of H_2O molecules due to the polarization, as shown in the NES spectrum of water as a result of measurement for 1 year. The window of transparency of the Earth atmosphere for the electromagnetic radiation in the middle IR-range almost covers NES-spectrum of water. Arrows A and B designate the energy of hydrogen bonds among individual H_2O molecules. Arrow C designates the energy at which the human body behaves itself as absolute black body (ABB) at optimum temperature 36.6°C and adsorbs the thermal radiation. A horizontal arrow designates the window of transparency of the earth atmosphere for the electromagnetic radiation in the middle IR-range.

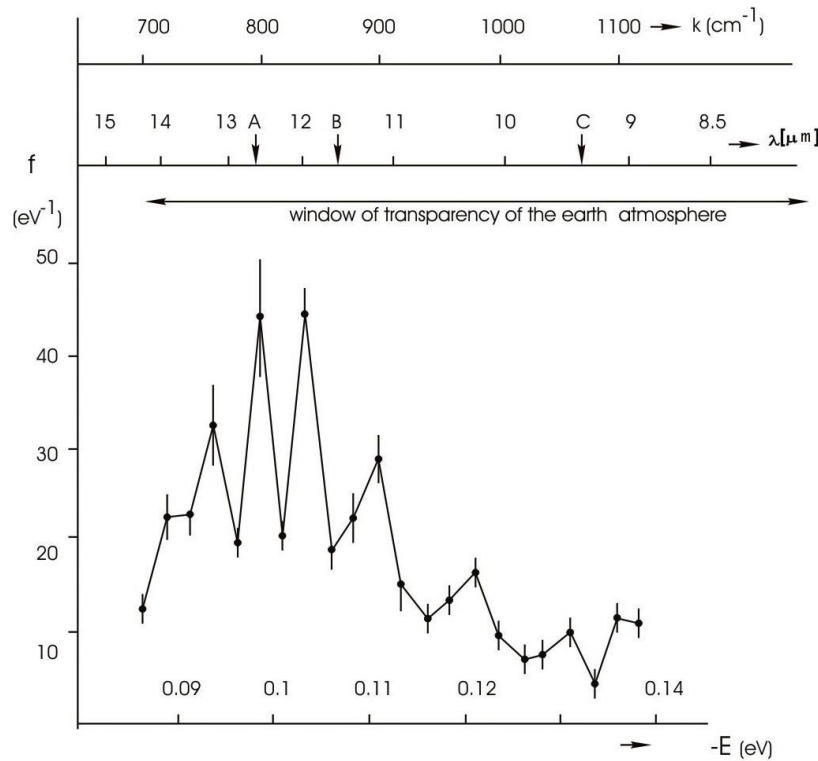


Figure 12. NES-spectrum of water as a result of measurement for 1 year (chemical purity - 99.99%, pH - 6.5-7.5, total mineralization - 400 mg/l, conductivity - 10 mk ·S/cm): λ – wavelength, k – wave number

These data indicate that the origination of life and living matter depends on the structural and physical-chemical properties of water, as well as its temperature and pH value. According to these terms the most satisfies to these conditions was interacting with CaCO_3 hot mineral water enriched with HCO_3^- and

Ca²⁺. Then, follows seawater. In the warm or hot mineral waters the peaks in DNES spectra were more pronounced when compared with the peaks obtained in the same water samples under a lower temperature. It indicates on more higher energy for existing of self-organized structures in time. Spectral range was within the middle-IR range from $\lambda = 8$ to $\lambda = 14$ μm . It is known that in that IR range exists a “window” of transparency of the Earth atmosphere towards electromagnetic radiation.

Conclusions

The data obtained suggest the possibility of application of the selective gas discharge in modeling non-equilibrium conditions with gas electric discharge simulating electrical spark discharge processes going on in primary atmosphere. In this process, within a thin layer of air border with 100 μm occurs the formation of reactive radicals interacting with each other to form new compounds (electrosynthesis). Such extreme conditions supposedly might take place in the primary anoxic Earth hydrosphere, consisting of a mixture of water and gases - H₂, CH₄, NH₃ и CO, subjected to the action of high-energy electrical discharges (lightning). The experiments showed that the most favorable for the emergence of life and maintenance of biochemical reactions is hot mineral water interacting with CaCO₃.

Acknowledgements

The authors wish to thank M. Chakarova from Bulgarian Academy of Sciences for registering IR-spectra.

References:

- Antonov, A. & Yuskeselieva, L. (1968) Research of water drops with high-frequency electric discharge (Kirlian) effect. *Bulgarian Academy of Science*, 21(5): 34–36.
- Antonov, A. & Yuskesselieva, L. (1985) Selective high frequency discharge (Kirlian effect). *Acta Hydrophysica*, Berlin, 5: 29.
- Antonov, A. (1995) Research of the non-equilibrium processes in the area in allocated systems. Dissertation thesis “Doctor of physical sciences”, Blagoevgrad, Sofia.
- Antonov, A. & Galabova, T. (1992) Reports from the 6th Nat. Conference of Biomedical Physics and Engineering. Sofia.
- Arunan E., Desiraju G.R., Klein R.A. et all. (2011) Definition of the hydrogen bond. *Pure Appl. Chem.*,83(8): 1637–1641.
- Bartha F., Kapuy O., Kozmutza C & Van Alsenoy C. (2003) Analysis of weakly bound structures: hydrogen bond and the electron density in a water dimer. *J. Mol. Struct. (Theochem)*, 666: 117–122.
- Fox, S.W. & Krampitz, G. (1964) Catalytic decomposition of glucose in aqueous solution by thermal proteinoids. *Nature*, 203: 1362–1364.
- Fox, S.W. & Wang, C.T. (1968) Melanocytestimulating hormone: Activity in thermal polymers of alpha-amino acids. *Science*, 160: 547–548.
- Goryainov S.V. (2012) A model of phase transitions in double-well Morse potential: Application to hydrogen bond. *Physica B*, 407, 4233–4237.
- Gudakova, G.Z. (1988) Study of parameters of gas discharge glow microbiological cultures. *Journal for*

Applied Spectroscopy, 49(3): 56–59.

Harada, I. & Fox, S.W. (1964) Thermal synthesis of natural amino-acids from a postulated primitive terrestrial atmosphere. *Nature*, 201: 335–336.

Ignatov, I. (2010) Which water is optimal for the origin (generation) of life? *Euromedica*, Hanover. pp. 34–37.

Ignatov, I. & Tsvetkova, V. (2011) Water for the origin of life and informationability of water. Kirlian (electric images) of different types of water. *Euromedica*, Hanover, pp. 32–35.

Ignatov, I. (2012) Origin of life and living matter in hot mineral water. Conference on the Physics, Chemistry and Biology of Water, Vermont Photonics, USA, 2012. p. 67.

Ignatov, I. & Mosin, O.V. (2012) Kirlian effect in study the properties of biological objects and water. *Biomedical electronics*, 12: 13–21. [in Russian].

Ignatov, I. & Mosin, O.V. (2013a) Color coronal (Kirlian) spectral analysis in modeling of nonequilibrium conditions with the gas electric discharges simulating primary atmosphere. S. Miller's experiments. *Naukovedenie*, 3(16): 1–15 [in Russian] [Online] Available: URL: <http://naukovedenie.ru/PDF/05tvn313.pdf> (May 10, 2013).

Ignatov, I. & Mosin, O.V. (2013b) Structural mathematical models describing water clusters. *Mathematical theory and modeling*, 3(11): 72–87.

Ignatov, I. & Mosin, O.V. (2013c) Modeling of possible processes for origin of life and living matter in hot mineral and seawater with deuterium. *Journal of Environment and Earth Science*, 3(14): 103–118.

Ignatov, I. & Mosin, O.V. (2013d) Possible processes for origin of life and living matter with modeling of physiological processes of bacterium *Basillus subtilis* as model system in heavy water. *Journal of Natural Sciences Research*, 3(9): 65–76.

Ignatov, I. & Mosin, O.V. (2013e) Method for colour coronal (Kirlian) spectral analysis. *Biomedical Radio Electronics*, 1: 38–47 [in Russian].

Ignatov, I. & Mosin, O.V. (2013f) Origin of life and living matter in hot mineral water. *Naukovedenie*, 2(6): 1–19 [in Russian] [Online] Available: URL: <http://naukovedenie.ru/PDF/04tvn213.pdf> (February 13, 2013).

Ignatov, I. & Mosin, O.V. (2013g) Isotopic composition of water and its temperature in the evolutionary origin of life and living matter. *Naukovedenie*, 1(14): 1–16 [in Russian] [Online] Available: URL: <http://naukovedenie.ru/PDF/42tvn113.pdf> (February 13, 2013).

Ignatov, I. & Mosin, O.V. (2014) Modeling of Possible Conditions For Origin of First Organic Forms in Hot Mineral Water, *Journal of Medicine, Physiology and Biophysics*, 3: 1-14.

Ignatov, I. & Mosin, O. V. (2014) Modeling of Possible Processes for Origin of Life and Living Matter in Sea and Hot Mineral Water. Process of Formation of Stromatolites, *Journal of Medicine, Physiology and Biophysics*, 5: 23-46.

Ignatov, I., Mosin, O. V. (2014) Coronal Gas Discharge Effect in Modeling of Non-Equilibrium Conditions with Gas Electric Discharge Simulating Primary Atmosphere and Hydrosphere for Origin of Life and Living Matter, *Journal of Medicine, Physiology and Biophysics*, 5: 47-70.

Ignatov I., Mosin O.V. (2014) Coronal Effect in Modeling of Non-Equilibrium Conditions with the Gas Electric Discharge, Simulating Primary Atmosphere, *Nanotechnology Research and Practice*, Vol. 3, No. 3,

pp. 127-140.

Johnson, A.P., Cleaves, H.J., Dworkin, J.P., Glavin, D.P., Lazcano, A. & Bada, J.L. (2008) The Miller volcanic spark discharge experiment. *Science*, 322(5900): 404–412.

Kirlian, S.D. (1949) Method of photographing objects in the high-frequency electric discharge. auth. cert. USSR. 1949. № 106401.

Lapitskiy, V.N. & Pesotskaya, L.A. (2012) Estimation of influence of schungite room on the state of human health by the method of Kirlian. *Scientific Paper*, 11: 1–7.

Lazcano, A. & Bada, J.L. (2004) The 1953 Stanley L. Miller experiment: fifty years of prebiotic organic chemistry. *Origin of Life and Evolution of Biospheres*, 33(3): 235–242.

Marinov, M. & Ignatov, I. (2008) Color Kirlian spectral analysis. Color observation with visual analyzer. Hanover: Euromedica, pp. 57–59.

Miller, S.L. (1953) A production of amino acids under possible primitive earth conditions. *Science*, 117(3046): 528–5299.

Mulkidjanian, A.Y. & Galperin, M.Y. (2009) On the origin of life in the Zinc world. Validation of the hypothesis on the photosynthesizing zinc sulfide edifices as cradles of life on Earth. *Biology Direct*, 4: 26–28.

Nakashima, T. (1987) Metabolism of proteinoid microspheres / Ed. T. Nakashima. In: Origins of life and evolution of biospheres, 20(3–4), pp. 269–277.

Nikolis, P. & Prigozhin, I. (1979) Self-organization in non-equilibrium systems. Moscow: Mir, pp. 1–512 [in Russian].

Pehek J.O., Kyler H.J. & Faust D.L. (1976) Image modulatic corona discharge photography. *Science*, 194(4262): 263–270.

Skarja, M., Berden, M. & Jerman, I. (1988) The influence of ionic composition of water on the corona discharge around water drops. *Journal of Applied Physics*, 84(5): 2436–2442.

Sugawara, T. (2011) Self-reproduction of supramolecular giant vesicles combined with the amplification of encapsulated DNA. *Nature Chemistry*, 1127: 775–780.

Wilson, A.T. (1960) Synthesis of macromolecules. *Nature*, 188: 1007–1009.

The IISTE is a pioneer in the Open-Access hosting service and academic event management. The aim of the firm is Accelerating Global Knowledge Sharing.

More information about the firm can be found on the homepage:

<http://www.iiste.org>

CALL FOR JOURNAL PAPERS

There are more than 30 peer-reviewed academic journals hosted under the hosting platform.

Prospective authors of journals can find the submission instruction on the following page: <http://www.iiste.org/journals/> All the journals articles are available online to the readers all over the world without financial, legal, or technical barriers other than those inseparable from gaining access to the internet itself. Paper version of the journals is also available upon request of readers and authors.

MORE RESOURCES

Book publication information: <http://www.iiste.org/book/>

Academic conference: <http://www.iiste.org/conference/upcoming-conferences-call-for-paper/>

IISTE Knowledge Sharing Partners

EBSCO, Index Copernicus, Ulrich's Periodicals Directory, JournalTOCS, PKP Open Archives Harvester, Bielefeld Academic Search Engine, Elektronische Zeitschriftenbibliothek EZB, Open J-Gate, OCLC WorldCat, Universe Digital Library, NewJour, Google Scholar

